BIOORGANIC CHEMISTRY **23,** 227–255 (1995)

Oxidation Chemistry of 5-[[3-(2-Amino-2-carboxyethyl)-5-hydroxy-1*H*-indol-4-yl]oxy]-[3-(2-amino-2-carboxyethyl)]-1*H*-indole: A Putative Aberrant Metabolite of 5-Hydroxytryptophan

ZHENG WU, XUE-MING SHEN, AND GLENN DRYHURST[1]

Department of Chemistry and Biochemistry, University of Oklahoma, Norman, Oklahoma 73019

Received May 12, 1995

Oxidative damage is known to occur in certain regions of the brain in a number of neurodegenerative disorders that include Alzheimer's Disease (AD) and transient cerebral ischemia and as a result of methamphetamine abuse. Furthermore, aberrant but unknown oxidized forms of 5-hydroxytryptophan (5-HTPP) and 5-hydroxytryptamine (5-HT) have been detected in the cerebrospinal fluid (CSF) of AD patients but not in that of age-matched controls. Accordingly, it is possible that aberrant oxidative metabolites of 5-HTPP and 5-HT might play roles in the neurodegenerative processes that occur in the AD brain and other neurodegenerative disorders. Previous studies have established that the title compound (**1**) is among the products of the electrochemically driven and various enzyme-mediated oxidations of 5-HTPP. This investigation has focused on both the electrochemical and peroxidase-mediated oxidations of **1** at physiological pH and has established that this dimer is significantly more easily oxidized than 5-HTPP from which it is derived. Under weakly oxidizing conditions **1** is oxidized via a putative carbocation intermediate to an equimolar mixture of 5-HTPP and tryptophan-4,5-dione (**2**). Under more strongly oxidizing conditions further oxidation of 5-HTPP gives a C(4)-centered carbocation intermediate that can react with the free hydroxyl residue of **1** to form a trimer, tetramer, and larger oligomers that are subsequently further oxidized ultimately to dione **2.** When administered into the brains of mice, **1** is a remarkably lethal compound (LD_{50} = 3.3 μg) and evokes a hyperactivity syndrome. Analyses of the brains of mice during this behavioral response reveal that an acute dose of **1** evokes a significant decrease of norepinephrine (NE) levels. Only minor alterations in whole brain levels of DA and 5-HT occur but levels of 3,4-dihydroxyphenylacetic acid, homovanillic acid, and 5-hydroxyindole-3-acetic acid are significantly elevated. These results suggest that the hyperactivity syndrome evoked by **1** is related to the elevated release and turnover of NE, DA, and 5-HT. Based upon the results obtained and by comparison with other pharmacologic manipulations that evoke a similar hyperactivity syndrome in mice and rats it appears that **1** might be metabolized *in vivo* to metabolites that interact with certain 5-HT and perhaps other receptor subpopulations.

Alzheimer's Disease (AD) is a neurodegenerative brain disorder of insidious onset and inexorable progression that affects approximately 15% of the population over the age of 65 years. The fundamental mechanisms that initiate and propagate the neuronal degeneration that occurs in the AD brain are unknown. However, neurons that die in AD involve many different neurotransmitter systems but only in remarkably selective anatomic regions of the brain. These include neurons that

[1] To whom correspondence should be addressed.

0045-2068/95 $12.00

are located entirely within the association areas of the cortex, the hippocampus, and amygdala and others that project from subcortical cell bodies and connect to one or more of the latter structures (*1*). Thus, serotonergic, noradrenergic, and cholinergic neurons with cell bodies located in the raphe nuclei, rostral areas of the locus ceruleus, and the nucleus basalis of Meynert, respectively, which project to and innervate vulnerable regions of the cortex and hippocampus are among pathways that degenerate in the AD brain (*1*). This selective pattern of damage argues against a random appearance of brain lesions and points to a progression of degeneration from defined starting points along specific connected neuronal pathways, i.e., a system neurodegeneration (*2*). Long serotonergic neurons that project from the raphe nuclei to the cortex and hippocampus may be among the pathways that begin to degenerate early in the progression of AD (*1, 3–6*). Saper *et al* (*2*) have proposed that the system neurodegeneration that occurs in AD might reflect the transfer of a pathogen(s) between neurons and that the selectivity of the neuronal degeneration results from the connectivity between affected neuronal pathways. Hardy *et al.* (*7*) have taken this idea a step further and suggested that AD is initiated by some form of chronic attack on the axon terminals of long serotonergic and noradrenergic neurons that project from the brain stem at points where they innervate blood capillaries in the association areas of the cortex and hippocampus. This chronic attack was speculated to be caused by an environmental toxicant, virus, or an autoimmune response (*7*). In essence, such a system neurodegeneration concept implies that a toxin enters serotonergic and noradrenergic terminals via blood capillaries and evokes a retrograde degeneration of these and connected neurons by transneuronal transfer of the toxin. This concept provides an elegant rationale for the selectivity of the neurodegeneration that occurs in the AD. However, evidence for the actual involvement of a specific environmental toxicant, virus, or other such pathogen in AD is lacking.

Many lines of evidence indicate that significant levels of oxidative damage occur in certain regions of the AD brain (*8–13*). Furthermore, using high-performance liquid chromatography (HPLC) with electrochemical detection, evidence has been obtained for the presence of aberrant although unknown oxidized forms of 5-hydroxytryptamine (5-HT; serotonin) and its precursor 5-hydroxytryptophan (5-HTPP) in the cerebrospinal fluid (CSF) of AD patients but not in that of age-matched controls (*14*). Taken together, these observations might indicate that aberrant oxidative transformations of endogenous indoles such as 5-HT and 5-HTPP occur in the AD brain. This laboratory is currently exploring the hypothesis that such reactions might lead to the formation of endotoxins that play roles in the degeneration of specific serotonergic and anatomically connected pathways that occurs in the AD brain. Similar hypotheses have been advanced to explain the damage that occurs in other neurodegenerative brain disorders. For example, methamphetamine (MA) abuse has been linked to aberrant oxidative transformations of 5-HT (*15*) and dopamine (DA) (*16*) to toxic metabolites that contribute to the degeneration of serotonergic, dopaminergic, and other neuronal pathways in the brain (*17–19*). Similarly, elevated rates of intraneuronal oxidation of DA (*20, 21*) and aberrant oxidation reactions of this neurotransmitter (*22*) have been linked to the degeneration of nigrostriatal dopaminergic neurons in idiopathic Parkinson's

Disease. Accordingly, the fundamental oxidation chemistry and biochemistry of 5-HT (*23–25*), 5-HTPP (*26–28*), and other indoles (*29*) endogenous to the brain has been studied in some detail. The principal goals of these studies were to isolate and identify reactions products, i.e., putative aberrant oxidative metabolites of these indolic compounds. Subsequent studies are now aimed at investigating the toxicity and other neuropharmacological and chemical properties of these putative aberrant metabolites in the brains of laboratory animals. (*30, 31*).

The electrochemically driven and various enzyme-mediated oxidations of 5-HTPP at physiological pH appear to proceed by similar chemical pathways to yield rather complex mixtures of products (*28*). One of these products is the dimer 5-[[3-(2-amino-2-carboxyethyl)-5-hydroxy-1*H*-indol-4-yl]oxy]-[3-(2-amino-2-carboxyethyl)]-1*H*-indole (**1**) (*28*). Preliminary studies revealed that **1** is remarkably lethal when administered into the brains of laboratory mice. Furthermore, it was discovered that at physiologically relevant concentrations (<50 μM) **1** exhibited a voltammetric oxidation peak having a peak potential (E_p) at pH 7.4 at more negative

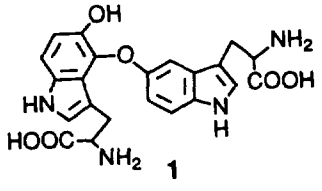

1

potentials than 5-HTPP from which it is derived. Similarly, **1** was very readily oxidized in reactions mediated by peroxidase/H_2O_2, tyrosinase/O_2, and ceruloplasmin/O_2. These observations suggested that under pathological conditions where 5-HTPP might be oxidized dimer **1** would be expected to undergo further oxidative transformations. This in turn suggested that the toxicity and behavioral responses evoked by central administration of **1** might be related to its *in vivo* oxidation. In this communication, therefore, the electrochemically driven and enzyme-mediated oxidation chemistry of **1** are described. Additionally, the *in vivo* properties of this dimer in terms of the behavioral response evoked following intracerebral administration, toxicity, and its short-term effects on various neurotransmitters/metabolites are reported.

EXPERIMENTAL

Chemicals

L-5-Hydroxytryptophan (5-HTPP), peroxidase (type VI from horseradish; EC 1.11.1.7), and 3-[*N*-morpholino]propanesulfonic acid (MOPS) were obtained from Sigma (St. Louis, MO) and were used without additional purification. HPLC grade acetonitrile (MeCN) was obtained from Fisher Scientific (Springfield, NJ). The concentrations of stock solutions of hydrogen peroxide (H_2O_2) were determined by iodometric titration using sodium thiosulfate as titrant and starch solution as

the indicator (*32*). The thiosulfate solution was standardized against potassium dichromate.

Apparatus and Methods

Voltammograms were obtained at a pyrolytic graphite electrode (PGE; Pfizer Minerals, Pigments and Metals Division, Easton, PA) having an approximate surface area of 4 mm^2. The fabrication and resurfacing procedures employed with the PGE have been described in detail elsewhere (*33*). A conventional three-electrode voltammetric cell containing a platinum wire counterelectrode and a saturated calomel reference electrode (SCE) was employed. Both linear sweep and cyclic voltammograms were obtained with a BAS-100A electrochemical analyzer (Bioanalytical Systems, West Lafeyette, IN). All voltammograms were corrected for iR drop. Controlled potential electrolyses were carried out with a Brinkman Instruments (Westbury, NY) Model LT73 potentiostat and a three-compartment cell in which the working, counter, and reference electrode compartments were separated with a Nafion membrane (type 117, duPont Co., Wilmington, DE). The working electrode compartment had a capacity of 40 ml. The working electrode consisted of several plates of pyrolytic graphite having a total surface area of ca. 100 cm^2. The counter electrode was platinum gauze. All potentials are referenced to the SCE at ambient temperature (22 ± 2°C).

Analytical HPLC employed a Gilson (Middleton, WI) binary gradient system equipped with two Model 302 pumps (5-ml pump heads), a Waters Associates (Milford, MA) Model 440 uv detector set at 254 nm, a Rheodyne (Cotati, CA) Model 7125 injector equipped with a 2.0-ml sample loop, and a reversed phase column (Brownlee Laboratories, RP-18, 5 μm, 250 × 7 mm). Preparative scale HPLC employed a Gilson binary gradient system equipped with Model 305 and 306 pumps (25-ml pump heads), a Gilson Holochrome uv detector (254 nm), and a preparative reversed phase column (J. T. Baker, Phillipsburg, NJ; Bakerbond C_{18}, 10 μm, 250 × 21.2 mm). For preparative HPLC some samples (1–10 ml) were introduced onto the column via a Rheodyne 7125 injector equipped with a 10.0-ml sample loop. Larger volumes (10–250 ml) were introduced onto the column through one of the HPLC pumps.

Analytical HPLC method I was employed to investigate the optimal experimental conditions to oxidize 5-HTPP to **1** using peroxidase VI/H_2O_2 in pH 7.4 MOPS buffer. Two mobile phase solvents were employed. Solvent A was prepared by adding 10 ml of concentrated ammonium hydroxide solution (NH_4OH) to 4.0 liters of deionized water; the pH of this solution was adjusted to 3.8 with glacial acetic acid (HOAc). Solvent B was prepared by addition to 2.0 liters of solvent A to 2.0 liters of HPLC grade MeCN. The following gradient was employed: 0–1.0 min, 100% solvent A and a linear increase of flow rate from 2.0 to 3.5 ml min^{-1}; 1.0–12 min, linear gradient to 4% solvent B; 12–30 min, linear gradient to 24% solvent B.

Preparative HPLC method II was used to separate and prepare **1** from the oxidation product mixtures formed by peroxidase VI–H_2O_2 oxidation of 5-HTPP in pH 7.4 MOPS buffer. Solvents A and B were employed as the mobile phases with the following gradient: 0–1.0 min, 100% solvent A, linear increase of flow rate

from 10 to 15 ml min^{-1}; 1–10 min, linear gradient to 5% solvent B; 10–32 min, linear gradient to 28% solvent B; 32–33 min, linear gradient to 100% solvent B; 33–50 min, 100% solvent B.

Preparative HPLC method III was employed to purify the crude, freeze-dried **1** obtained using method II. Two mobile phase solvents were used. Solvent C was prepared by adding 10.0 ml of NH_4OH to 4.0 liters of deionized water; the pH of this solution was adjusted to 4.5 with HOAc. Solvent D was prepared by adding 400 ml of MeCN to 3600 ml of solvent C. The following gradient was used: 0–18 min, linear gradient from 100% solvent C to 100% solvent D at a flow rate of 10.0 ml min^{-1}; 18–26 min, 100% solvent D.

Preparative HPLC method IV was employed to desalt freeze-dried samples of **1** obtained using method IV. Two mobile phase solvents were used. Solvent E was deionized water. Solvent F was prepared by adding 2.0 liters of MeCN to 2.0 liters of deionized water. The following gradient was used: 0–6 min, 100% solvent E at a flow rate of 10.0 ml min^{-1}; 6–16 min, linear gradient to 100% solvent F; 16–24 min, 100% solvent F.

Analytical HPLC method V was employed to monitor the course of the peroxidase VI/H_2O_2 and electrochemical oxidations of **1** in pH 7.4 MOPS buffer. Mobile phase solvents A and B were used with the following gradient: 0–1 min, 100% solvent A and a linear gradient to 8.0% solvent B; 6–30 min, linear gradient to 26% solvent B; 30–36 min, linear gradient to 52% solvent B; 36–37 min, linear gradient to 100% solvent B; 37–47 min, 100% solvent B.

Preparative HPLC method VI was used to separate the products of both the peroxidase VI/H_2O_2 and electrochemical oxidation of **1** formed in pH 7.4 MOPS or phosphate buffers. Mobile phase solvents A and B were employed with the following gradient: 0–7 min, linear gradient from 0 to 12% solvent B at a flow rate of 10 ml min^{-1}; 7–22 min, linear gradient to 18% solvent B; 22–39 min, linear gradient to 50% solvent B; 39–40 min, linear gradient to 100% solvent B; 40–51 min, 100% solvent B.

Preparative HPLC method VII was used to desalt the freeze-dried oxidation products of **1** obtained using method VI. Solvent G was deionized water. Solvent H was prepared by adding 800 ml of deionized water to 3.2 liters of MeCN. The gradient employed was as follows: 0–6 min, 100% solvent G; 6–16 min, linear gradient to 100% solvent H; 16–24 min, 100% solvent H. The flow rate was constant at 10.0 ml min^{-1}.

Fast atom bombardment mass spectrometry (FAB-MS) was performed with a VG Instruments (Manchester, UK) ZAB-E mass spectrometer. ^1H and ^{13}C NMR spectra were obtained with either a Varian (Palo Alto, CA) XL-300 or a Varian XL-500 spectrometer. Ultraviolet–visible spectra were recorded on a Hewlett-Packard 8452A diode array spectrophotometer.

Analysis of in Vitro Reaction Products

The concentrations of **1–4** and 5-HTPP in various oxidation product mixtures were determined from calibration curves (peak height versus concentration) obtained using known concentrations of each compound with HPLC method VI.

Dione **2** cannot be isolated as a pure solid. Accordingly, **2** was prepared by controlled potential electrooxidation of 5-HTPP (0.035 mM) at 700 mV in 0.01 M HCl. The resulting purple solution (100-ml aliquot) was then chromatographed using HPLC method VI when **2** eluted at a rentention time of ca. 19 min. The concentration of **2** was calculated on the basis of its molar absorptivity at 540 nm (1513 M^{-1} cm^{-1}). Appropriate dilutions of this solution with 0.01 M HCl were made.

Animals

Outbred adult male mice of the Hsd:ICR albino strain (Harlan Sprague–Dawley, Madison, WI) weighing 30 ± 3 g were used in all animal experiments. Animals were housed 10 per cage, allowed access to Purina Rat Chow and water *ad libitum*, and maintained on a 12-h light/dark cycle with lights on at 7:00 AM. No animals were used in experiments until at least 7 days after receipt from the supplier. Experimental animals, after light either anesthesia, were treated with 5 μl of isotonic saline (0.9% NaCl) containing **1** (free base) administered into the vicinity of the left lateral ventricle. Injections were accomplished freehand with a 10-μl microsyringe, the point of puncture being 2.9 mm anterior to the interaural line and 1.1 mm left lateral of the midline according to a modification (*30*) of the procedure of Lehman *et al.* (*34*). The injection at this point was perpendicular to the scalp to a depth of 3 mm. The depth of the injection was controlled by a collar on the needle of the syringe. The dose was injected over the course of ca. 10 s; the needle was held in place for an additional 10 s before removal. Control animals were treated with 5 μl of isotonic saline. The LD_{50} value, used as a measure of toxicity and defined as the dose of injected **1** (free base) in 5 μl of isotonic saline at which 50% of the treated animals died within 2 h, was determined by injecting doses ranging from 2 to 20 μg and using the statistical methods of Dixon (*35*, *36*).

In experiments designed to determine the effects of **1** on neurotransmitter/metabolite levels, animals were sacrificed by guillotine decapitation after predetermined times following administration of **1** (3.3 μg). Following sacrifice, the brain was rapidly removed from the skull cavity, weighed, and homogenized. The homogenization solution (10.0 ml/g of brain) contained 0.10 M NaH_2PO_4, 1.0 mM Na_2 EDTA, 1.0 mM octanesulfonic acid sodium salt, and 1.04 μM N_ω-methyl-5-hydroxytryptamine (N_ω-Met) in 30% aqueous MeCN. Citric acid was then added to adjust the pH of this solution to 4.0. N_ω-Met was employed as the internal standard for the determination of the biogenic amine neutrotransmitters and metabolites using HPLC with electrochemical detection (HPLC-EC). Homogenization was accomplished with 15 up/down strokes with a Teflon-coated glass Potter homogenizer. The homogenate was then centrifuged using a Beckman GS-15R centrifuge set at 14,000 rpm and 4°C for 45 min. The supernate was filtered through a 0.45-μm BAS (Bioanalytical Systems, West Lafayette, IN) polyacetate filter using low-speed centrifugation and was captured in a 1.5-ml polypropylene tube. The filtrate so obtained was stored at −80°C until required. The HPLC-EC procedure employed has been described in detail elsewhere (*37*). The concentrations of NE, DA, 5-HT and related metabolites in whole mouse brain were measured using 5.0-μl aliquots of the filtrate. Typical neurochemical concentrations found in whole brain analyses

of controls (nmol/g wet tissue, mean ±SE) were as follows: norepinephrine (NE), 2.62 ± 0.06; dopamine (DA), 6.96 ± 0.12; 3,4-dihydroxyphenylacetic acid (DOPAC), 0.80 ± 0.06; homovanillic acid (HVA), 1.20 ± 0.09; 5-HT, 4.19 ± 0.08; 5-hydroxyindole-3-acetic acid (5-HIAA), 1.66 ± 0.05. All animal procedures were approved by the Institutional Animal Use and Care Committee at the University of Oklahoma.

Synthesis of ***1***

5-HTPP (200 mg, 0.9 mmol) and peroxidase VI (1.0 mg) were dissolved in 100 ml of pH 7.4 MOPS buffer solution (0.1 M). After dissolution, 10.0 ml of 45 mM (0.45 mmol) hydrogen peroxide (H_2O_2) in water was added and the solution diluted to 250 ml with pH 7.4 MOPS buffer. After 1 h, the entire reaction solution was pumped onto the preparative reversed phase column and the products separated using HPLC method II. Compound **1** eluted at a retention time (t_R) of 28 min and was collected in a flask immersed in crushed dry ice. Following several replicate experiments the combined solutions containing **1** were shell frozen and freeze–dried. The resulting solid residue was dissolved in ca. 10 ml of deionized water and **1** (t_R = 20 min) was purified using HPLC method III. The solution eluted under the peak at t_R = 20 min was again collected in a flask immersed in a bed of dry ice and then freeze–dried. The resulting dry solid was dissolved in ca. 10 ml of deionized water and was desalted using HPLC method IV (t_R = 22 min). After freeze–drying **1** was obtained as a pure white fluffy solid, mp = 226°C (d). In pH 7.4 phosphate buffer **1** exhibited a uv spectrum with λ_{max}, nm (log ε_{max}, M^{-1} cm^{-1}) at 274 (4.03), 296 (4.10), and 222 (4.64). FAB-MS (3-nitrobenzyl alcohol matrix) gave *m/e* = 439.1682 (MH^+, 100%; $C_{22}H_{23}N_4O_6$; Calcd. *m/e* = 439.1618). ^1H NMR (D_2O) gave δ: 7.42 (d, $J_{6,7}$ = 8.7 Hz, 1H, C(7)-H), 7.33 (d, $J_{6',7'}$ = 8.7 Hz, 1H, C(7′)-H), 7.24 (s, 1H, C(2)-H), 7.17 (s, 1H, C(2′)-H), 7.01 (d, $J_{4,6}$ = 2.1 Hz, 1H, C(4)-H), 6.97 (d, $J_{6',7'}$ = 8.4 Hz, 1H, C(6′)-H), 3.91–3.85 (m, 2H, C(α)-H, C(α′)-H), 3.31–3.05 (m, 3H, C(β)-H_2, C(β′)-H), 2.85 (dd, *J* = 15.0 Hz, 9.9 Hz, 1H, C(β′)-H). These assignments were confirmed using homonuclear decoupling experiments. In the dark at −20°C **1** could be stored indefinitely. However, exposure to light at room temperature caused the dimer to slowly turn gray, indicative of its decomposition.

Isolation, Purification, and Structural Characterization of the Products of Peroxidase/H_2O_2-Mediated Oxidation of ***1***

In a representative experiment of 1.0 ml of 5.0 mM H_2O_2 (5.0 μmol) was added to 25.0 ml of pH 7.4 MOPS buffer solution (0.1 M) containing 11 mg of **1** (1.0 mM, 25 μmol) and 0.1 mg of peroxidase VI. Immediately upon addition of H_2O_2 the initially colorless solution became yellow. The yellow color faded within ca. 5 s and the solution became a pale purple color. After 5 min the entire reaction solution was pumped onto the preparative reversed phase column and the components of the mixture were separated using HPLC method VI. The chromatogram obtained exhibition five major peaks having t_R values of 8.8, 10.1, 13.4, 21.3, and 26.8 min and a smaller peak at t_R = 29.2 min. The peak at t_R = 13.4 min corresponded to unreacted **1.** The component eluted at t_R = 8.8 min was 5-HTPP identified by

comparison of its t_R, uv spectrum, and cyclic voltammetric behavior with that of the authentic compound.

Tryptophan-4,5-dione **(2)**

This purple compound eluted at t_R = 8.8 min (method V) and in the HPLC mobile phase (pH 3.8) exhibited a spectrum with λ_{max} = 540 and 352 nm. Compound **2** is a major product of the electrochemical oxidation of 5-HTPP at low pH and has been previously characterized as a quinoxaline derivative after trapping with *o*-phenylenediamine (*26*).

5-[[3-(2-Amino-2-carboxyethyl)-5-hydroxy-1H-indol-4-yl]oxy]-4-[[3-(2-amino-2-carboxyethyl)-1H-indol-5-yl]oxy]-tryptophan **(3)**

Compound **3** (t_R = 21.3 min, HPLC method V) was isolated as a white, fluffy, solid, mp = 210°C (d). In pH 7.4 phosphate buffer **3** exhibited uv bands at λ_{max}, nm (log ε_{max}, M^{-1} cm^{-1}) = 298 (4.32), 276 (4.40), and 224 (4.93). FAB-MS (3-nitrobenzyl alcohol matrix) gave *m/e* = 657.2355 (MH^+, 44%, $C_{33}H_{33}N_6O_9$; Calcd. *m/e* = 657.2309). Thus, **3** was a simple trimer of 5-HTPP having a molar mass of 656 g and a molecular formula $C_{33}H_{32}N_6O_9$. ^{13}C NMR (Me_2 SO-d_6) gave δ: 172.01, 171.95, 171.06, 158.40, 157.99, 152.96, 144.87 142.34, 135.54, 134.18, 132.77, 132.35, 127.19, 126.62, 125.70, 121.84, 121.56, 119.14, 115.16, 112.88, 111.20, 108.23, 108.00, 107.51, 106.67, 106.07, 105.40, 54.30, 53.50, 53.28, 28.30, 27.56, and 27.33. This spectrum showed the presence of three carbonyl (C=O) resonances (172.01–171.06), 24 aromatic carbon resonances (158.40–105.40), and 6 aliphatic carbon resonances (54.30–27.33) in agreement with proposed structure of **3.** The ^1H NMR spectrum of **3** (D_2O) at room temperature was poorly resolved. However, at 50°C δ: 7.73 (d, $J_{6',7'}$ = 8.7 Hz, 1H, C(7′)-H), 7.58 (s, 1H, C(2)-H), 7.55 (s, 1H, C(2′)-H), 7.41 (s, 1H, C(2″)-H), 7.55 (d, $J_{4'',6'}$ = 2.7 Hz, 1H, C(4′)-H), 7.53 (d, $J_{6,7}$ = 8.7 Hz, 1H, C(7)-H), 7.52 (d, $J_{6'',7''}$ = 9.0 Hz, 1H, C(7″)-H), 7.31 (dd, $J_{4',6'}$ = 2.4 Hz, $J_{6',7'}$ = 8.7 Hz, 1H, C(6′)-H), 7.20 (d, $J_{6'',7''}$ = 8.7 Hz, 1H, C(6″)-H), 6.94 (d, J = 9.0 Hz, 1H, C(6)-H), 4.32 (dd, J = 5.1, 9.9 Hz, 1H, C(α)-H), 4.21 (dd, J = 5.1, 8.1 Hz, 1H C(α′)-H), 4.16 (dd, J = 5.1, 8.7 Hz, 1H, C(α″)-H), 3.63–3.20 (m, 6H, C(β)-H_2, C(β′)-H_2, C(β″)-H_2. ^1H NMR (Me_2 SO-d_6) showed, in addition to the above resonances, δ: 10.89 (s, 1H), 10.82 (s, 1H), and 10.75 (s, 1H), corresponding to the N(1)-H, N(1′)-H, and N(1″)-H protons. Homonuclear decoupling and two-dimensional correlated spectroscopy (COSY) experiments revealed that the following resonances were coupled: 7.73 (C(7′)-H) with 7.31 (C(6′)-H), 7.55 (C(4′)-H) with 7.31 (C(6′)-H), 7.52 (C(7″)-H) with 7.20 (C(6″)-H), 7.53 (C(7)-H) with 6.94 (C(6)-H).

5-[[3-(2-Amino-2-carboxyethyl)-5-[[3-(2-amino-2-carboxyethyl)-5-hydroxy-1H-indol-4-yl]oxy]-1H-indol-4-yl]oxy]-4-[[3-(2-amino-2-carboxyethyl]-1H-indol-5-yl]-tryptophan **(4)**

Compound **4** (t_R = 26.8 min, HLPLC method V) was isolated as a white, fluffy solid; mp = 204°C(d). In pH 7.4 phosphate buffer the uv spectrum of **4** exhibited bands at λ_{max}, nm (log ε_{max}, M^{-1} cm^{-1}) 298 (4.33), 276 (4.40), and 224 (4.93). FAB-

MS (3-nitrobenzyl alcohol matrix) gave *m/e* = 875.2947 (MH^+, 9%, $C_{44}H_{43}N_8O_{12}$; Calcd. *m/e* = 875.3000). Thus, **4** had a molar mass of 874 g and a molecular formula $C_{44}H_{42}N_8O_{12}$ corresponding to a tetramer of 5-HTPP. ^{13}C NMR (Me_2 SO-d_6) gave δ: 172.60, 172.44, 171.62, 171.26, 158.67, 158.26, 153.86, 153.31, 145.58, 145.20, 142.34, 142.00, 134.78, 134.47, 133.16, 132.84, 128.22, 127.35, 127.04, 126.56, 126.13, 122.45, 122.14, 119.67, 115.68, 113.46, 111.83, 111.70, 111.37, 110.13, 108.56, 107.70, 107.09, 106.62, 106.23, 106.05, 55.04, 54.41, 53.73, 53.07, 28.95, 28.50, 27.98, and 27.68. This spectrum thus showed the presence of four carbonyl (C = 0) resonances (172.60–171.26), 32 aromatic carbon resonances (158.67–106.05), and 8 aliphatic carbon resonances (55.04–27.68) in agreement with the conclusion that is a tetramer of 5-HTPP. The ^1H NMR (D_2O), 50°C) spectrum of **4** gave δ: 7.61 (d, *J* = 8.67 Hz, 1H), 7.56 (s, 1H), 7.53 (s, 1H), 7.50 (d, *J* = 9.6 Hz, 1H), 7.48 (s, 1H), 7.45 (d, *J* = 9.0 Hz, 1H), 7.18 (d, *J* = 8.6 Hz, 2H), 6.79 (d, *J* = 8.7 Hz, 1H), 7.40–7.20 (unresolved peaks, 4H), 4.6–2.5 (unresolved multiplets, 12H). ^1H NMR (Me_2 SO-d_6) gave δ: 11.02 (s, 1H, N-H), 10.98 (s, 1H, N-H), 10.94 (s, 1H, N-H), 10.71 (s, 1H, N-H) in addition to the largely unresolved aromatic and aliphatic resonances.

5-[[3-(2-Amino-2-carboxyethyl)-5-[[3-(2-amino-2-carboxyethyl)-5-hydroxy-1H-indol-4-yl]oxy]-1H-indol-4-yl]oxy]-4-[[3-(2-amino-2-carboxyethyl)-4-[[3-(2-amino-2-carboxyethyl)-1H-indol-5-yl]oxy]-1H-indol]5-yl]oxy-tryptophan **(5)**

Compound **5** (t_R = 29.2 min, HPLC method V) was isolated as a white fluffy solid. In the HPLC mobile phase (pH 3.8) **5** exhibited uv bands at λ_{max} = 300, 276 nm. FAB-MS (thioglycerol/glycerol/TFA matrix) gave a pseudomolecular ion (MH^+) at *m/e* = 1093 (1%). Thus this compound was a simple pentamer of 5-HTPP having a molar mass of 1092 g and molecular formula $C_{55}H_{52}N_{10}O_{15}$. It was not possible to isolate sufficient quantities of **5** in a reasonable amount of time to permit a ^{13}C NMR spectrum and its ^1H NMR spectrum between ca. 7–7.8 ppm and 4–2 ppm was too complex to be resolved.

RESULTS

Electrochemical Oxidation of **1**

Cyclic voltammograms of **1** dissolved in buffered aqueous solution at pH 7.4 at a sweep rate (v) of 10 mV s^{-1} are presented in Fig. 1. At low concentrations of **1** (e.g., 40 μM) oxidation peak I_a (E_p = 147 mV) and oxidation peak II_a (E_p = 287 mV) appear on the initial anodic sweep (Fig. 1A). Following scan reversal reduction peak III_c (E_p = −216 mV) appears. On the second anodic sweep oxidation peak III_a (E_p = −210 mV) forms a reversible couple with reduction peak III_c. The latter couple appeared even when the initial anodic sweep was reversed immediately after scanning through oxidation peak I_a (Fig. 1B). With increasing initial concentration of **1** (e.g., 200 μM, Fig. 1C; 400 μM, Fig. 1D) oxidation peak II_a grew relative to peak I_a with the result that the latter peak appeared as a shoulder on the former peak. However, after scan reversal, the peak III_c/peak III_a couple remained as a major feature of cyclic voltammograms. With increasing values of v the experimental

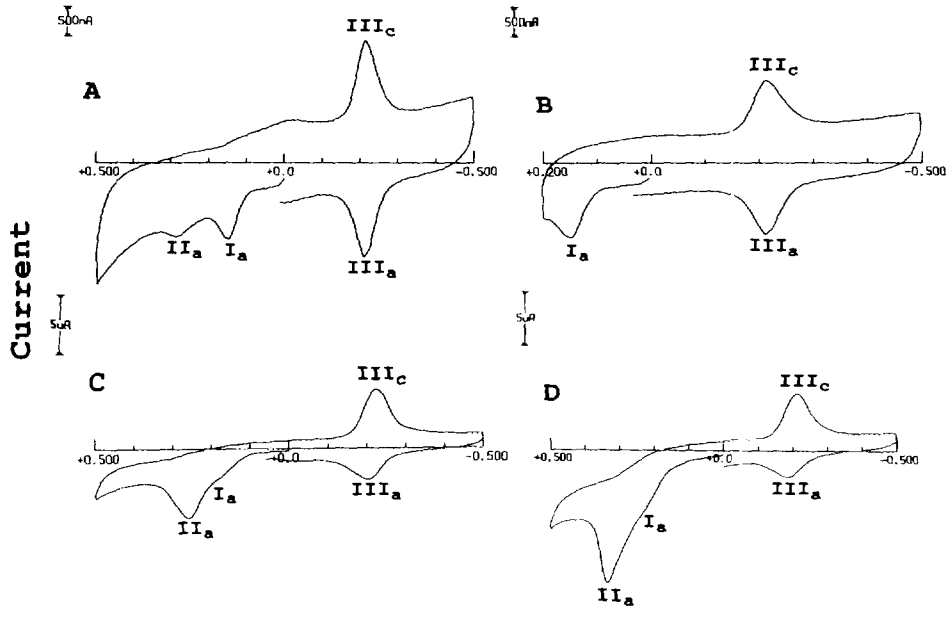

FIG. 1. Cyclic voltammograms at the PGE of (A and B) 40 μM **1**, (C) 200 μM **1**, and (D) 400 μM **1** in pH 7.4 phosphate buffer (μ = 1.0). Sweep rate, 10 mV s^{-1}.

peak function ($i_p/AC\nu^{1/2}$, all terms having their usual electrochemical significance) for peak I_a increased significantly. Thus, using 40 μM **1** and ν = 0.01, 0.1, 1.0, and 10.0 Vs^{-1}, the mean experimental peak current functions were 1.46, 3.07, 10.77, and 14.89 μA mm^{-2} mM$^{-1}\nu^{-1/2}$, respectively. These observations indicated that **1** was strongly adsorbed at the surface of the PGE and that peak I_a was largely under adsorption control.

Controlled potential electrooxidations of **1** at pH 7.4 using potentials ranging from 140 to 400 mV resulted in the development of a purple color in the initially colorless reaction solution. This purple color was more intense using more positive applied potentials and/or higher initial concentrations of **1**. A series of HPLC chromatograms (method VI) of the product solutions formed after controlled potential electrooxidation of **1** (400 μM) at applied potentials of 140 mV (Fig. 2A), 200 mV (Fig. 2B), and 400 mV (Fig. 2C) are presented in Fig. 2. The rate of electrooxida-

FIG. 2. HPLC chromatograms of the product solutions formed following controlled potential electrooxidation of 100 μM **1** at (A) 140 mV, (B) 200 mV, and (C) 400 mV in pH 7.4 phosphate buffer (μ = 0.1). Electrolyses were terminated after transfer of approximately 1 faraday per mole of **1**. HPLC employed method VI. Injection volume, 2.0 ml.

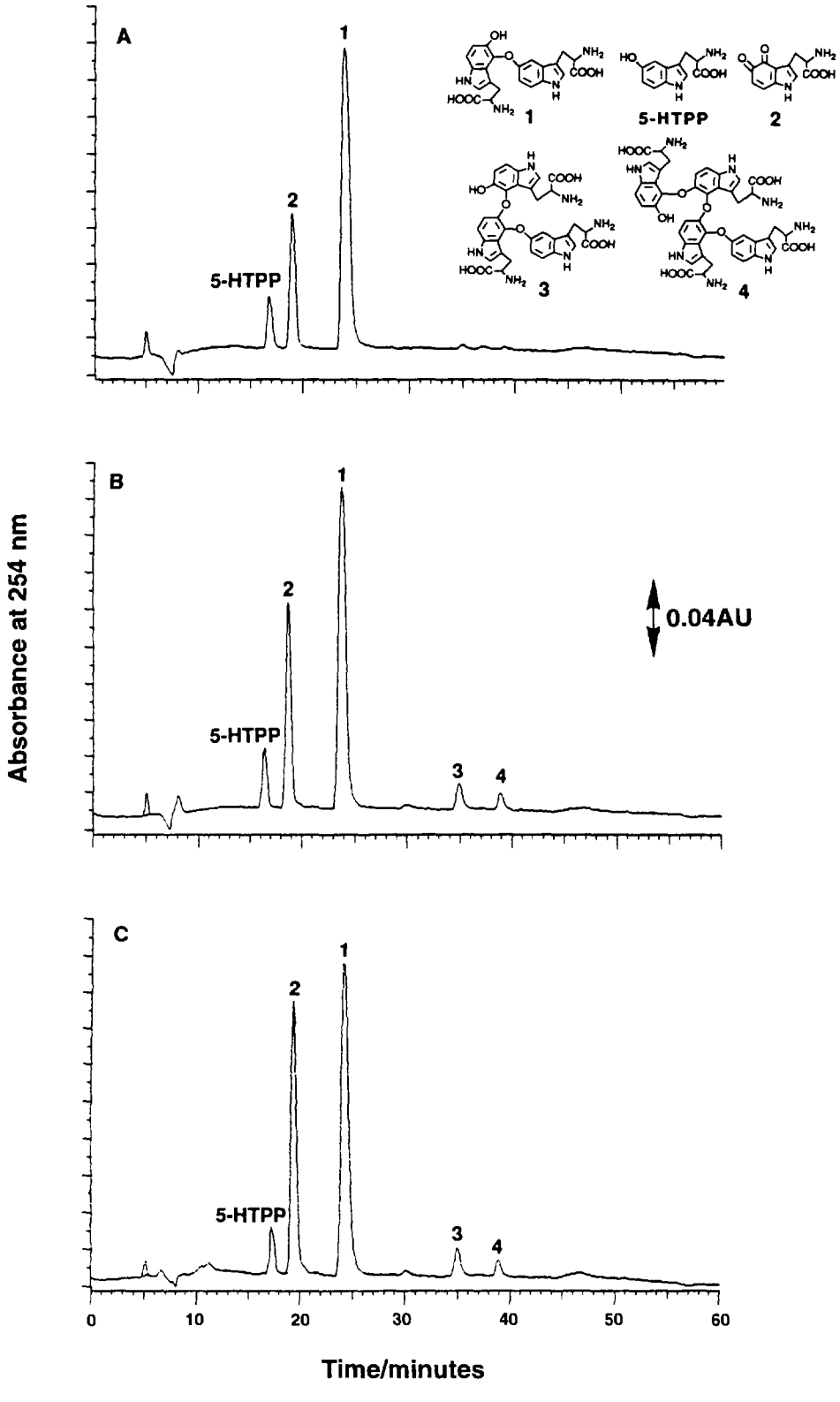
A
1
2
5-HTPP
1
5-HTPP
2
3
4
B
1
2
5-HTPP
3
4
0.04AU
C
1
2
5-HTPP
3
4
0
10
20
30
40
50
60
Time/minutes
Absorbance at 254 nm

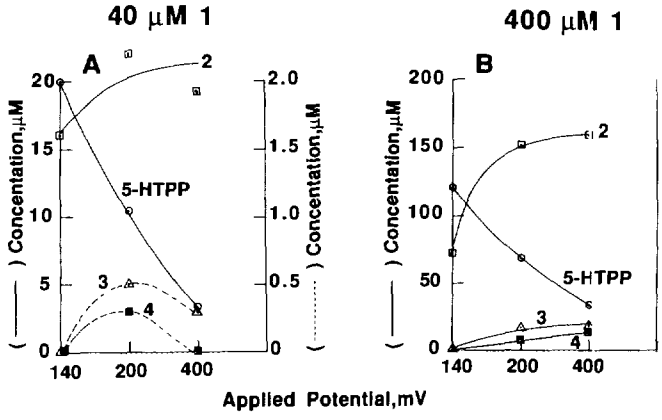

FIG. 3. Yields of products formed upon controlled potential electrooxidation of (A) 40 μM **1** and (B) 400 μM **1** in pH 7.4 phosphate buffer (μ = 0.1) as a function of applied potential. Electrolyses were terminated after the transfer of approximately 1 faraday per mole of **1**. Data based on HPLC analysis of product solutions (method VI).

tion of **1** increased significantly with increasingly positive applied potentials. Furthermore, at applied potentials ≥200 mV the product profile and yields changed throughout the course of the electrolysis. Accordingly, for comparative purposes the chromatograms shown in Fig. 2 were recorded after transfer of approximately 1 faraday per mole of **1** oxidized. Under these conditions, controlled potential electrooxidation of **1** at 140 mV (i.e., corresponding to the rising portion of oxidation peak I_a) gave two products, tryptophan-4,5-dione (**2**) and 5-HTPP. Exhaustive electrolyses of **1** (40, 100, 400 μM) at 140 mV also gave **2** and 5-HTPP as the sole reaction products. At applied potentials ≥200 mV trimer **3** and tetramer **4** appeared as products in addition to **2** and 5-HTPP (Figs. 2B, 2C). However, at applied potentials ≥250 mV, **3**, **4**, and 5-HTPP appeared as products in the early stages of the reaction but with continued electrolysis their yields decreased and ultimately these compounds disappeared giving dione **2** as the sole reaction product.

The influence of the applied potential on the yields of **2**, 5-HTPP, **3**, and **4** when the electrolysis of **1** (40 μM) was terminated after transfer of 1 faraday per mole of the dimer is shown in Fig. 3A. At an applied potential of 140 mV 5-HTPP and dione **2** are the sole reaction products in approximately equimolar yield. It should be noted that the yields of **2** shown in Fig. 3 and elsewhere in this communication were always underestimated because of the instability of this dione at pH 7.4, an effect which became more pronounced with increasing concentration. This was because of the tendency of **2** to form unknown, insoluble, and apparently polymeric products. With increasingly positive applied potentials the yields of 5-HTPP systematically decreased, indicating that this compound was further oxidized. Correspondingly, the yields of **2** increased. At an applied potential of 200 mV trimer **3** and tetramer **4** appeared as products in very low yields when very dilute solutions of **1** (40 μM) were electrolyzed (Fig. 3A). With increasingly positive applied potentials

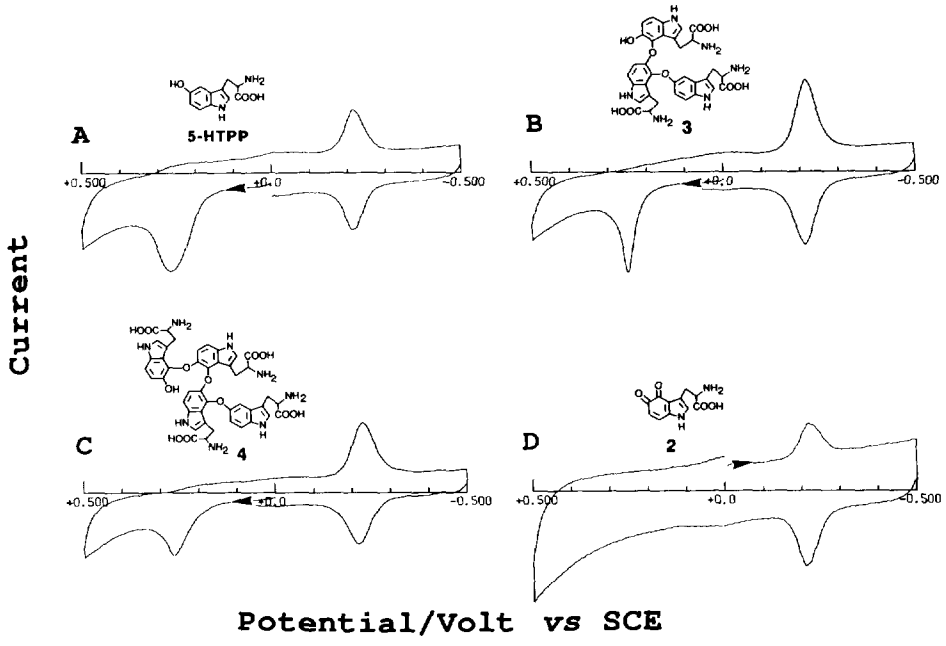

FIG. 4. Cyclic voltammograms at the PGE of ca. 40 μM solutions of (A) 5-HTPP, (B) **3**, (C) **4**, and (D) **2** in pH 7.4 phosphate buffer (μ = 0.1). Sweep rate, 10 mV s^{-1}.

(e.g., 400 mV) the yields of **3** and **4** decreased. Controlled potential electrooxidation of higher concentrations of **1** (400 μM) at 140 mV also gave dione **2** and 5-HTPP as the sole products (Fig. 3B). Again, at more positive applied potentials the yield of 5-HTPP decreased and that of **2** increased. However, the yields of **3** and **4** were more than 20 times higher than observed following electrolyses of 40 μM **1** and increased with increasingly positive applied potentials. However, at applied potentials ≥250 mV, **3**, **4**, and 5-HTPP ultimately disappeared and the sole product was dione **2**.

The results presented in Fig. 3 imply that at potentials ≥250 mV, 5-HTPP, **3**, and **4**, formed as a result of the electrooxication of **1**, undergo secondary oxidation reactions. Cyclic voltammograms (ν = 10 mV s^{-1}) of 5-HTPP, **3**, and **4** (40 μM) at pH 7.4 confirm that these oxidations in fact must occur (Fig. 4). Thus, on the initial anodic sweep 5-HTPP, **3** and **4** exhibited voltammetric oxidation peaks having E_p values of 273, 250, and 264 mV, respectively. Cyclic voltammograms of **1** (40 μM; ν = 10 mV s^{-1}; Fig. 1A) exhibited oxidation peak II_a at E_p = 287 mV. Because 5-HTPP at the same concentration exhibited an oxidation peak at almost the same potential (Fig. 4A) and is the major product (with **2**) of the peak I_a oxidation of **1** (Fig. 3A) it can be concluded that 5-HTPP is the species predominantly responsible for peak II_a.

Cyclic voltammograms of 5-HTPP, **3**, and **4** all exhibit a reversible couple at $E^{\circ\prime}$ = −216 ± 7 mV (Figs. 4A–4C) corresponding to dione **2** (Fig. 4D). Thus, the

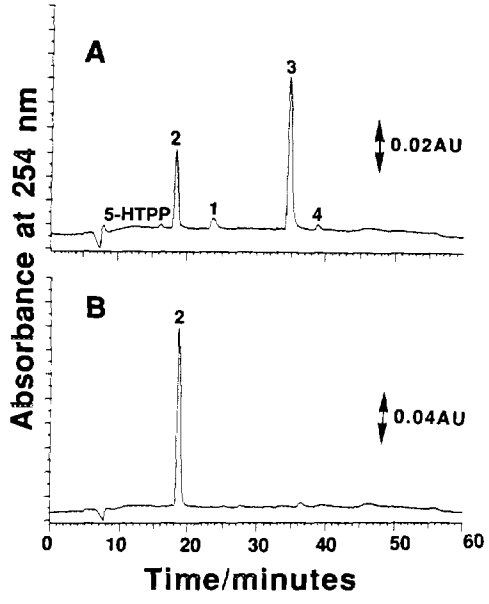

FIG. 5. HPLC chromatograms of the product solutions formed following controlled potential electrooxidation (400 mV) of 40 μM solutions of trimer **3** in pH 7.4 phosphate buffer (μ = 0.1) after (A) 1 min and (B) 60 min. Chromatography employed HPLC method VI. Injection volume, 2.0 ml.

latter dione is not only formed as a result of the peak I_a electrooxidation of **1** (Figs. 1B, 3) but also as a result of the peak II_a oxidations of 5-HTPP, **3,** and **4.**

Figure 5A shows a chromatogram (method VI) of the product solution formed following controlled potential electrooxidation (400 mV) of trimer **3** (40 μM) for 1 min. Thus, during the initial stages of the reaction 5-HTPP, **2, 1,** and tetramer **4** are formed. However, with continued electrolysis 5-HTPP, **1** and **4** disappear and **3** is ultimately oxidized to dione **2** (Fig. 5B). With increasing concentrations of **3** the initial yields of 5-HTPP, **1,** and **4** are appreciably higher. However, the ultimate product of the electrolysis continues to be **2.** Similarly, controlled potential electrooxidations of tetramer **4** at ≥250 mV initially yield 5-HTPP, **2, 1,** and **3** but with continued electrolysis dione **2** was the sole product of this reaction.

Peroxidase/H_2O_2-Mediated Oxidation of **1**

Upon addition of H_2O_2 (8 μM) to a solution of **1** (20 μM) dissolved in buffered aqueous solution at pH 7.4 containing peroxidase (0.5 units ml^{-1}) the initially colorless solution immediately turned yellow and subsequently (≤5 s) a purple color developed. Repetitive rapid scanning uv–visible spectrophotometry (240–700 nm; 20-s scan intervals) revealed the appearance, growth, and decay of an intermediate (λ_{max} = 420 nm) that subsequently transformed in part into dione **2** (λ_{max} = 540, 354 nm). A chromatogram (method VI) of the product solution formed after incubation (5 min) of **1** (20 μM) in the presence of peroxidase (0.5 units ml^{-1}) and